5.15

KINETIC THEORY AND SIMULATION OF SINGLE-CHANNEL WATER TRANSPORT

Emad Tajkhorshid, Fangqiang Zhu, and Klaus Schulten
Theoretical and Computational Biophysics Group, Beckman Institute for Advanced Science and Technology, University of Illinois at Urbana-Champaign, Urbana, IL 61801, USA

Water translocation between various compartments of a system is a fundamental process in biology of all living cells and in a wide variety of technological problems. The process is of interest in different fields of physiology, physical chemistry, and physics, and many scientists have tried to describe the process through physical models. Owing to advances in computer simulation of molecular processes at an atomic level, water transport has been studied in a variety of molecular systems ranging from biological water channels to artificial nanotubes. While simulations have successfully described various kinetic aspects of water transport, offering a simple, unified model to describe trans-channel translocation of water turned out to be a nontrivial task.

Owing to its small molecular size and its high concentration in the environment, water is able to achieve significant permeation rates through different membranes, including biological cell membranes which are primarily composed of lipid bilayers. As such, water is generally exchangeable between various compartments of living organisms. However, due to the hydrophobic nature of the core of lipid bilayers, high permeation rates can only be achieved through devising additional pores in the bilayer that increase the permeability of water. These pores, known as channels, are primarily formed by folding and aggregation of one or more polypeptide chains inside the membrane. Aquaporins (AQPs) are the most prominent family of biological channels that facilitate transport of water across membranes in a selective manner. Other porins and channels also allow water molecules to pass, but they are either nonselective channels or mainly used for transport of other substrates, i.e., water is co-transported with other substrates through these channels.

S. Yip (ed.),
Handbook of Materials Modeling, 1797–1822.

Water permeation through biological channels, such as AQPs, has been the subject of theoretical and experimental studies for many years [1]. Molecular dynamics (MD) simulations provide an ideal tool for investigating water transport through channels [2–5], since the movement of every single water molecule can be closely monitored in the simulations. A large body of evidence, including the recently solved structures of these channels and extensive MD simulations, have indicated that the pore region of selective water channels confines water molecules to a single file configuration, in which a highly correlated motion of neighboring, hydrogen-bonded water molecules governs the rate of diffusion and permeation of water through the channel. A very similar behavior of water has been reported in artificial water channels formed by carbon nanotubes (CNTs).

This chapter presents a detailed description of water motion and permeation through water channels, through a comprehensive survey of the theory associated with single-channel water transport, methodologies developed to simulate such events, and comparison of experimental and calculated observables. The main objective is to provide the reader with a clear description of experimentally measurable properties of water channels. Our description links these properties to the microscopic structure and dynamics of channels. We show how observables like channel permeabilities can be examined by computer simulations and we present a mathematical theory of single-channel water transport.

1. Structurally Known Biological Water Channels

AQPs are a family of membrane water channels for which crystallographic structures are available. They are present in nearly all life forms. In human, AQPs have been found in multiple tissues, such as the kidneys, the eye, and the brain. They form homo-tetramers in cell membranes, each monomer forming a functionally independent water pore, which does not conduct protons, ions or other charged solutes (Fig. 1a). A fifth pore, formed in the center of the tetramer, has been proposed to conduct ions under certain circumstances [6]. However, passive transport of water across cell membranes remains to be the main established physiological function of AQPs.

Atomic resolution structures of aquaporin-1 (AQP1) [7–9] and the *E. coli* glycerol channel (GlpF) [10] have been employed in MD simulations characterizing the structure–function relationship of these channels in particular, regarding their selectivity [2–4, 11–14].

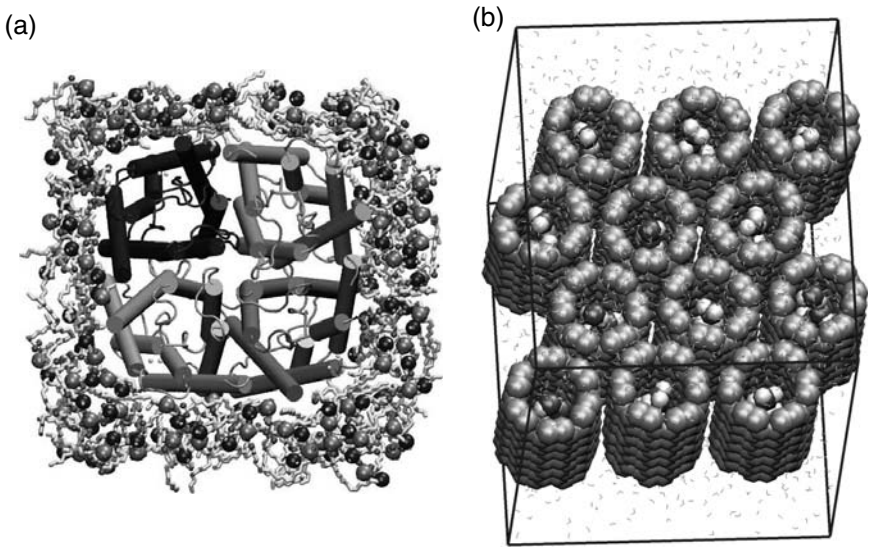

Figure 1. (a) Top view of a tetrameric AQP surrounded by lipidmolecules of a membrane. Each monomer constitutes an independent water pore. (b) An array of CNTs as a simplified model for the study of single channel water transport.

2. Nanotubes as Simple Models of Water Channels

Synthetic pore-forming molecules, such as nanotubes, have attracted a great deal of attention recently. Due to their chemical simplicity, these artificial channels have been the subject of numerous experimental and theoretical studies [15, 16]. Simulation studies have employed CNTs as models for complicated biological channels, as they can be investigated more readily by MD simulations [17, 18] due to their simplicity, stability, and small size (Fig. 1b).

Biological water channels are much more complex than CNTs, with irregular surfaces and highly inhomogeneous charge distributions. For example, MD simulations have revealed that water molecules in AQPs adopt a bipolar orientation which is induced electrostatically and is linked to the need that proton conduction must be prevented in AQP channels [3]. CNTs are electrically neutral, and may not reproduce some important features of biological channels. However, one may modify CNTs through the introduction of charges [18] to mimic various aspects of biological water channels.

Computational studies have suggested that CNTs can be designed as molecular channels to transport water. Single-walled CNTs (with a diameter of 8.1 Å) have been studied recently by MD simulations. Simulations revealed that the CNTs spontaneously fill with a single file of water molecules and that water diffuses through the tube concertedly at a fast rate.

3. Experimental Measurement of Transmembrane Water Transport

The key characteristics accounting for transport through water channels are the *osmotic permeability* (p_f) and the *diffusion permeability* (p_d) [1], both measurable experimentally. p_f is measured through application of osmotic pressure differences, while p_d is measured through isotope labeling, e.g., use of heavy water. In this section, we explain how water transport is characterized experimentally, and what are the most important properties used to characterize the rate of transport of water through channels. We will introduce and define p_f and p_d of water channels, and, in particular, investigate the relationship between the two for single-file water channels.

When the solutions on the two sides of a membrane have different concentrations of an impermeable solute, water flows from the low concentration side to the other side. In dilute solutions, the net water flux through a single-water channel, j_W (mol/s), is linearly proportional to the solute concentration difference ΔC_S (mol/cm^3):

$$j_W = p_f \Delta C_S, \tag{1}$$

where ΔC_S (mol/cm^3) is the concentration difference of the impermeable solute between the two reservoirs connected by the channel, j_W (mol/s) is the net molar water flux through the channel, and p_f (cm^3/s) is defined as the *osmotic permeability* of the channel [1].

In contrast, no net water flux is expected in equilibrium, i.e., when no solute concentration difference is present. It is, however, still of interest to study water diffusion through the channels for $\Delta C_S = 0$. For this purpose, experiments have been designed where a fraction of water molecules is labeled, e.g., by isotopic replacement or by monitoring nuclear spin states, so that they can be traced. Assuming that the interactions of these so-called *tracers* with the membrane and with other water molecules are identical to those of normal water molecules, tracers can be used to study diffusion of water molecules through channels at equilibrium conditions.

When the reservoirs on the two sides of a membrane have different concentrations of tracers, a diffusional tracer flux will be established down the concentration gradient, although the average net water flux (consisting of both tracers and normal water molecules) remains zero. The tracer flux j_{tr} (mol/s) through a single channel is linearly proportional to the tracer concentration difference ΔC_{tr} (mol/cm^3):

$$j_{tr} = p_d \Delta C_{tr}, \tag{2}$$

where p_d (cm^3/s) is defined as the *diffusion permeability* of the channel [1] (Fig. 2).

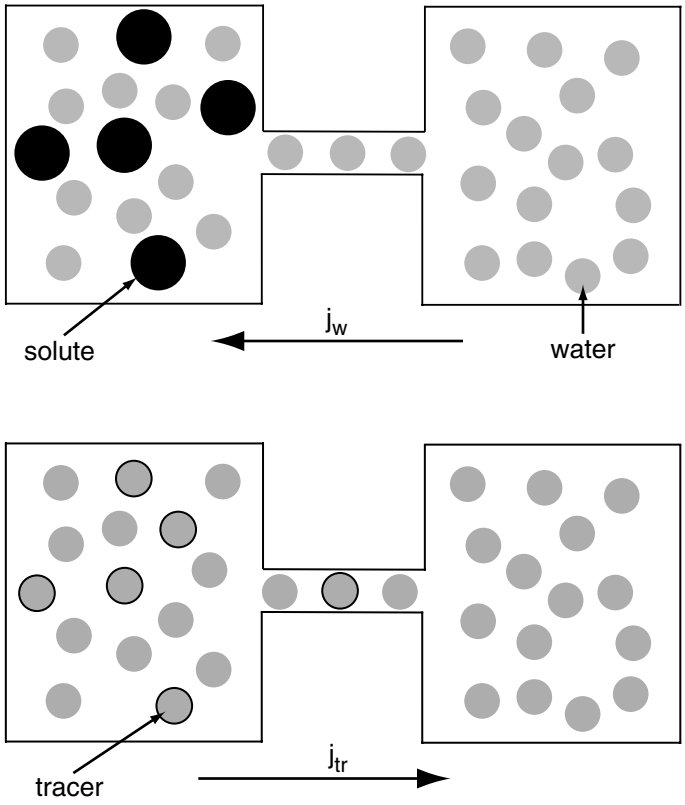

Figure 2. Schematic presentation of experimental procedures to measurediffusion and osmotic permeability of channels. (Top) Addition of an impermeable solute to one side of the channel establishes a chemical potential difference of water that drives water transport to the solute-rich side. (Bottom) In the absence of a chemical potential difference of water across the channel, labeled water molecules (tracers) can be used to monitor random diffusion of water from one side to the other side of the channel.

Different experimental techniques are used for measurement of P_f and P_d [19]. It is important to note that, due to difficulties in measuring water transport through single channels, almost all of the experimental setups measure water permeation through a membrane, and the measured permeabilities (P_f and P_d with capital P) are those of the entire membrane. To obtain single-channel permeabilities, p_f or p_d, one needs to know the density of the channel in the membrane, i.e., the number of channels per unit area. However, the ratio p_f/p_d can be measured without the knowledge of the channel density [20].

P_d is measured in the absence of a chemical potential difference of water (balanced osmotic/hydrostatic pressure on the two sides of the membrane). There is no net transport of water under these conditions. In order to monitor

random translocation of water molecules from one side to the other side of the membrane, special water molecules (*tracers*) are needed. Isotopic water (such as ^3H_2O) or water molecules with different nuclear spin states can be used for this purpose. Immediately after introduction of tracers, tracer concentrations of the two reservoirs are monitored directly or indirectly over time [19], and P_d can be determined from the decay rate of the concentration difference.

P_f is usually measured in the presence of an osmotic pressure difference, i.e., a difference in solute concentration. Typical P_f measurements are performed on cells or liposomes (small lipid vesicles with embedded water channels), by exploiting the stopped-flow technique. In this setup, the solute concentration of the extracellular solution is suddenly changed, resulting in volume changes of the cells (or vesicles) due to the net water flux. The volume change can be inferred by monitoring light scattering from the suspension [21], and the net water flux determined from the rate of volume change. P_f for a planar membrane can be determined by measuring the ionic concentration distribution near the surfaces of the membrane [22].

4. Theory of Single-file Water Transport

The theory and derivations presented in this section closely follow Zhu *et al.* [5, 23]. We define a *permeation event* as a complete transport of a water molecule through the channel from one reservoir to the other. Let q_0 be the average number of such permeation events in one direction per unit time; the number of permeation events in either direction should be identical, resulting in a total number of $2q_0$. q_0 is an intrinsic property of a water channel and is independent of tracer concentration.

Let us assume that one reservoir has a tracer concentration of C_{tr}, and (for the sake of convenience) that the other reservoir has zero tracer concentration. The ratio of tracers to all water molecules in the first reservoir is C_{tr}/C_W, where $C_W = 1/V_W$ is the concentration of water, and V_W (18 cm^3/mol) is the molar volume of water, which is usually assumed to be constant. Since according to our assumption tracers move just like normal water molecules, the same proportion (i.e., C_{tr}/C_W) should characterize water molecules permeating the channel. Consequently, the tracer flux can be related to the total number of water molecules permeating the channel (q_0) by $j_{tr} = (1/N_A)q_0(C_{tr}/C_W)$, where N_A is Avogadro's number. Therefore, p_d and q_0 are related by a constant factor:

$$p_d = \frac{V_W}{N_A} q_0 = v_W q_0, \tag{3}$$

where $v_W = V_W/N_A$ is the average volume of a single water molecule.

Within narrow channels water molecules form a single file, and their movement along the channel axis accordingly is highly correlated. Recently, a continuous-time random-walk (CTRW) model was proposed [24] to describe the transport of single-file water in channels. This model assumes that the channel is always occupied by N water molecules, and the whole water file moves in hops (translocations that shift all water molecules by the distance separating two neighboring water molecules) simultaneously and concertedly, with leftward and rightward hopping rates k_l and k_r, respectively. In equilibrium, k_l and k_r have the same value, denoted as k_0. Due to strong coupling between the water molecules, local effects (energetic barriers arising from interaction with certain parts of the channel wall, access resistance at channel entrances, etc.) contribute to the hopping rate of the whole water file. Consequently, all factors affecting the kinetics of water movement are effectively integrated into this single parameter (k_0). In the following, we will show that both p_d and p_f can be predicted by this model, in terms of N and k_0.

Since the complete permeation of a water molecule from one end of the channel to the other end includes at least $N + 1$ hops (shifts) of the single file, one expects the rate of permeation events at equilibrium to be smaller than the hopping rate. Indeed, the number of uni-directional permeation events per unit time, q_0, is given by

$$q_0 = \frac{k_0}{N+1}. \tag{4}$$

Equation (4) has been proven from kinetics [24] as well as using a state diagram [18], and its validity was verified by MD simulations of CNTs [17, 18]. Combining Eqs. (3) and (4), p_d can be expressed as:

$$p_d = \frac{v_W k_0}{N+1}. \tag{5}$$

p_f is measured when a net water flux is induced by different solute concentrations in two reservoirs. In this case, the chemical potentials of water in the two reservoirs are different (the difference denoted as $\Delta\mu$). Consequently, the hopping rates (k_r and k_l) of the two directions are no longer the same. We note that the yield of a hop is the transfer of one water molecule from one reservoir to the other, resulting in a free energy change of $\Delta\mu$ in the system. In analogy to the forward and backward rates of a chemical reaction, the ratio of k_r to k_l can be expressed by [25]:

$$k_r/k_l = \exp\left(\frac{-\Delta\mu}{k_B T}\right), \tag{6}$$

where k_B is the Boltzmann constant and T is the temperature.

We note now that k_r and k_l are both functions of $\Delta\mu/k_B T$. Since under physiological conditions, $\Delta\mu$ is much smaller than $k_B T$ (e.g., $\Delta\mu/k_B T = 0.0036$

for a 200 mM solution of sucrose, according to Eq. (10)), we can expand k_r and k_l to first order:

$$k_r = k_0 \left(1 + \alpha \frac{\Delta\mu}{k_B T}\right), \quad k_l = k_0 \left(1 + \beta \frac{\Delta\mu}{k_B T}\right) \tag{7}$$

(for a symmetric channel also holds $\alpha = -\beta$). The net water flux can be expressed by the difference between k_r and k_l:

$$j_W = \frac{1}{N_A}(k_r - k_l) = \frac{k_0(\alpha - \beta)}{N_A} \frac{\Delta\mu}{k_B T}. \tag{8}$$

Substituting Eq. (7) into Eq. (6) and comparing the first order terms in $\Delta\mu / k_B T$ leads to $\beta - \alpha = 1$. The net water flux is then:

$$j_W = -\frac{k_0}{N_A} \frac{\Delta\mu}{k_B T}. \tag{9}$$

For dilute solutions, $\Delta\mu$ is linearly proportional to the solute concentration difference [1]:

$$\Delta\mu = -k_B T V_W \Delta C_S. \tag{10}$$

From Eqs. (9) and (10), we obtain

$$j_W = k_0 v_W \Delta C_S \tag{11}$$

and using Eq. (1),

$$p_f = v_W k_0. \tag{12}$$

According to Eqs. (5) and (12), the ratio of p_f to p_d predicted by the CTRW model is

$$p_f / p_d = N + 1. \tag{13}$$

The difference between p_f and p_d can be further elaborated as follows. For single-file water transport, a hop results in the net transfer of one water molecule from one side of the channel to the other side. p_f is related to the rate of net water transfer under a chemical potential difference and, therefore, is determined by the hopping rate (see Eq. (12)). In contrast, p_d is determined by the rate of permeation events (see Eq. (3)). A permeation event requires an individual water molecule to traverse all the way through the channel, and is *not* the same as a hop. Actually, the p_f / p_d ratio is exactly determined by the relative rates of hops and permeation events. Most models proposed for single-file water transport predict this ratio to be N or $N + 1$ [1].

As stated before, most experimental techniques take advantage of osmotic pressure to establish a chemical potential difference that is needed for the determination of p_f. A hydrostatic pressure difference ΔP between the two

reservoirs can also give rise to a difference in the chemical potential of water [1]

$$\Delta\mu = v_{\mathrm{W}}\Delta P. \tag{14}$$

In fact, the *osmotic pressure* difference between two solutions is defined as the hydrostatic pressure difference that would generate the same $\Delta\mu$. Therefore, the osmotic pressure difference between two dilute solutions is given by van't Hoff's law [1]:

$$\Delta P = RT\Delta C_{\mathrm{S}}, \tag{15}$$

where $R = k_{\mathrm{B}}N_{\mathrm{A}}$ is the gas constant. It is also known experimentally that equal osmotic and hydrostatic pressure differences produce the same water flux through water channels [19]. The hopping rates and, hence, the water flux are functions of $\Delta\mu$ alone (Eqs. (7) and (9)), regardless of whether $\Delta\mu$ arises from osmotic or hydrostatic pressure differences.

According to the CTRW model, when an osmotic or hydrostatic pressure difference exists, the water file performs a biased random walk, characterized by the hopping rates k_{r} and k_{l}. In this section, we will determine the statistical distribution of hops as a function of time.

Within any infinitesimally small time $\mathrm{d}t$, the probability of the water file to make a rightward hop is $k_{\mathrm{r}}\,\mathrm{d}t$, independent of its history, i.e., when and how many rightward hops were made before. Such a process is referred to as a *Poisson process*, and the total number of rightward hops within time t, $m_{\mathrm{r}}(t)$, obeys the well-known *Poisson distribution*, whose mean and variance are both $k_{\mathrm{r}}t$. Similarly, the number of leftward hops, $m_{\mathrm{l}}(t)$, also obeys the Poisson distribution, with $k_{\mathrm{l}}t$ being its mean and variance.

The net number of hops, $m(t)$, is defined as the difference of the numbers of rightward and leftward hops, i.e., $m(t) = m_{\mathrm{r}}(t) - m_{\mathrm{l}}(t)$. Since the probabilities of making rightward and leftward hops are independent of each other, we obtain:

$$\langle m(t)\rangle = (k_{\mathrm{r}} - k_{\mathrm{l}})t, \tag{16}$$

$$\mathrm{Var}[m(t)] = (k_{\mathrm{r}} + k_{\mathrm{l}})t, \tag{17}$$

where $\mathrm{Var}[m] = \langle m^2\rangle - \langle m\rangle^2$. Equations (16) and (17) show that both the mean and the variance of $m(t)$ increase linearly with time. These expressions show that monitoring the average number of hops and its variance permits one to determine both k_{r} and k_{l} [5].

5. Collective Diffusion Model of Single-channel Water Transport

Following its definition, p_f is measured in experiments under nonequilibrium conditions, for systems with nonzero $\Delta\mu$. In principle, the same conditions (a chemical potential difference across the channel) can be established in MD simulations of water transport. Two of the techniques for doing so are (1) introduction of solutes to one side of the membrane to generate an osmotic pressure difference [25], and (2) application of a hydrostatic pressure difference across the channel through mechanically manipulating individual water molecules in the bulk [4, 5]. Through adjustment of the salt concentration or of the pressure difference, one may reach different values of $\Delta\mu$ in the simulations. Due to the presently accessible (ns) time scale of MD simulations, however, one has to adopt a large $\Delta\mu$ to obtain sufficient statistics of water permeation. This leads to situations that are far from actual experimental conditions, and it is not clear whether the results represent the normal kinetics of the water channel under study. If one can establish a quantitative relationship between water conduction under equilibrium and nonequilibrium conditions, this problem can be circumvented. In this section we demonstrate that water permeation obeys a linear current – $\Delta\mu$ relationship over a very wide range of $\Delta\mu$ values and that equilibrium MD simulations ($\Delta\mu = 0$) can be used to characterize the osmotic permeability of a channel.

Water permeation usually involves multiple water molecules in a channel whose movements are coupled to each other. As a result, a complicated multidimensional representation seems to be necessary to model this process. In the following, we introduce a collective coordinate, n, which offers a much simplified description of water translocation in channels. The derivation follows closely Zhu *et al.* [23].

Consider a channel (of length L) aligned along the z-direction. The collective coordinate n is defined in its differential form as follows: let $S(t)$ denote the set of water molecules in the channel at time t, and let us assume that the displacement of water molecule i in the z-direction during $\mathrm{d}t$ is $\mathrm{d}z_i$; then we define

$$\mathrm{d}n = \sum_{i \in S(t)} \frac{\mathrm{d}z_i}{L}. \tag{18}$$

By demanding $n = 0$ at $t = 0$, $n(t)$ can be uniquely determined by integrating $\mathrm{d}n$. Note that $S(t)$ changes with time, and that a water molecule i contributes to n only when it is in the channel, i.e., if $i \in S(t)$ at time t. We further note that every water molecule crossing the channel from one reservoir to the other contributes to n a total increment of exactly $+1$ or -1. Therefore, n quantifies the net amount of water permeation, and the trajectory $n(t)$ describes the time evolution of the permeation.

An important scenario is the stationary state in which a steady water flux through the channel exists. In this case, $n(t)$ on average grows linearly with t, and the water flux is given by

$$j_{\mathrm{W}} = \frac{1}{N_{\mathrm{A}}} j_n = \frac{1}{N_{\mathrm{A}}} \frac{\langle n(t) \rangle}{t}, \tag{19}$$

where N_{A} is Avogadro's number, and $j_n = N_{\mathrm{A}} j_{\mathrm{W}}$ is the water flux in the unit of number of water molecules/s.

At equilibrium, the net amount of water permeation through the channel vanishes on average, i.e., $\langle n(t) \rangle = 0$. Spontaneous, random water transport, however, may occur due to thermal fluctuation. Such microscopic fluctuations may not be detectable in experiments, but can be readily observed in MD simulations through $n(t)$. At equilibrium, $n(t)$ can be described as a one-dimensional unbiased random walk, with a diffusion coefficient D_n that obeys

$$\left\langle n^2(t) \right\rangle = 2 D_n t. \tag{20}$$

D_n has dimension t^{-1} since n is dimensionless. Intuitively, D_n is related to the rate at which the net transport of one water molecule happens spontaneously. All factors affecting water kinetics contribute to D_n and are effectively integrated into this single parameter.

In the presence of a chemical potential difference ($\Delta\mu$) of water between the two reservoirs, n obeys a biased random walk. We note that the net transport of one water molecule from one reservoir to the other results in a change of $\pm\Delta\mu$ in the free energy, and that the total free energy change is proportional to the net amount of water transported. The free energy can be expressed then as a linear function in n:

$$U(n) = \Delta\mu n. \tag{21}$$

Consequently, the trajectory of n can be described as a one-dimensional diffusion in a linear potential. Therefore, on average n is drifting with a constant velocity [23]:

$$\langle n(t) \rangle = -\frac{\Delta\mu}{k_{\mathrm{B}} T} D_n t, \tag{22}$$

which corresponds to a stationary water flow through the channel. According to Eq. (19), the water flux is given by

$$j_n = -\frac{\Delta\mu}{k_{\mathrm{B}} T} D_n. \tag{23}$$

From Eqs. (1), (10), (19) and (23) one obtains then for the osmotic permeability of the channel

$$p_{\mathrm{f}} = v_{\mathrm{W}} D_n. \tag{24}$$

Equation (24) shows that one can determine p_f using the D_n value obtained from equilibrium MD simulations (cf. Eq. (20)) [23].

The CTRW model proposed for single-file water channels assumes that the whole water file moves in discrete hops simultaneously and concertedly, with rightward and leftward hopping rates k_r and k_l, respectively. k_0, defined as the value of k_r or k_l at equilibrium, is the major kinetic parameter in the model. Since each hop changes the collective coordinate, n, by $+1$ or -1, it holds $n(t) = m_r(t) - m_l(t)$, where $m_r(t)$ and $m_l(t)$ are the number of rightward and leftward hops during time t, respectively. Because $m_r(t)$ and $m_l(t)$ obey a Poisson distribution (see also above) whose mean and variance are both $k_0 t$ at equilibrium [5], one obtains $\langle n^2(t) \rangle = 2k_0 t$. Comparison with Eq. (20) yields $D_n = k_0$. Therefore, for the discrete water movement described by the CTRW model, D_n is identical to the hopping rate k_0, and the expression derived from the CTRW model, namely, $p_f = v_W k_0$ [5], is actually equivalent to Eq. (24) in the collective diffusion model [23]. However, while the CTRW model is only valid for single-file channels, the collective diffusion model is applicable to any water channel since it makes no assumption regarding water configuration or water movement inside the channel.

In the CTRW model, in order to determine the net water flux ($j_n = k_r - k_l$) as a function of $\Delta\mu$, the rate theory expression $k_r/k_l = \exp(-\Delta\mu/k_B T)$ was exploited [5, 25], along with the linear response approach which assumes that $\Delta\mu$ is much smaller than $k_B T$ [5]. The model, however, is not able to predict how j_n relates to $\Delta\mu$ when $\Delta\mu$ is comparable or larger than $k_B T$. In contrast, the collective diffusion model (Eq. (23)) predicts a linear relationship between j_n and $\Delta\mu$ even when $\Delta\mu$ exceeds $k_B T$ [23].

6. Simulation of Water Transport and Calculation of p_d and p_f

Equilibrium MD simulations provide an ideal tool to study free water diffusion through channels, since all water molecules can be easily traced in the simulations, and q_0 counted [3, 23]. p_d can then be calculated according to Eq. (3) from the simulations. In order to determine p_f in a fashion similar to experiments, one needs to produce different osmotic or hydrostatic pressures on the two sides of the membrane.

Figure 3 illustrates a scheme to induce a hydrostatic pressure difference in MD simulations [4, 5]. In order to avoid inaccuracies at the boundaries, applying periodic boundary conditions has become a common practice in MD simulation of molecular systems, particularly those that involve a considerable amount of solvents like water. In a periodic system, the unit cell is replicated in three dimensions; therefore, water layers and membranes alternate along the z-direction, defined as the membrane normal. Figure 3 shows a water layer

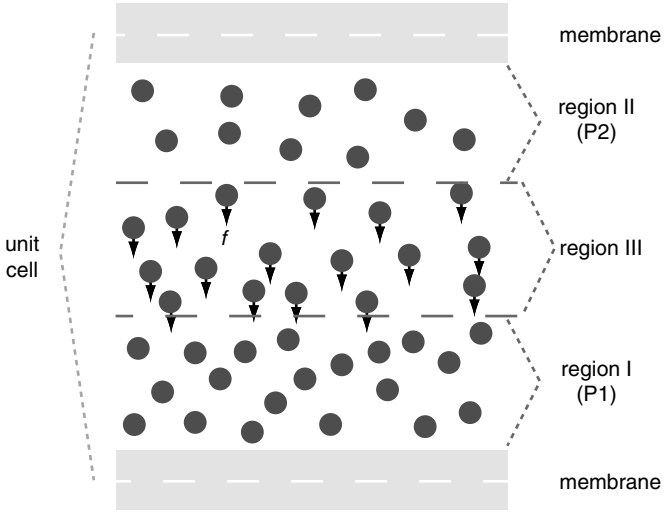

Figure 3. Illustration of the method to produce a pressuredifference in MD simulations. The two membranes shown in the figure are "images" of each other under periodic boundary conditions. A constant force f is applied only to water molecules in region III.

sandwiched by adjacent membranes. We define three regions (I, II, III) in the water layer, as shown in the figure. Region III is isolated from the two sides of the membrane by regions I and II, respectively. A constant force f along the z-direction is exerted on all water molecules in region III, generating a pressure gradient in this region that, consequently, results in a pressure difference between regions I and II, i.e., on the two sides of the membrane [4]

$$\Delta P = P_1 - P_2 = \frac{nf}{A}, \tag{25}$$

where n is the number of water molecules in region III, and A the area of the membrane. Consequently, a net water flux j_W through the membrane channels embedded in the membrane can be induced, and p_f calculated from j_W and ΔP. We note that the membrane needs to be held in its position, e.g., by constraints, to prevent an overall translation of the whole system along the direction of the applied forces.

Assuming that the thickness of region III is d, the number of water molecules in this region is $n = Ad/v_W$. Substituting this into Eq. (25) and the result into Eq. (14), we obtain for the chemical potential difference of water between regions I and II:

$$\Delta\mu = fd. \tag{26}$$

The external force field generates a mechanical potential difference of fd between regions I and II, which must be exactly balanced by the chemical

potential difference $\Delta\mu$ under a stationary population distribution of water, therefore also giving Eq. (26).

In an earlier approach [4], all water molecules in the bulk region, including those adjacent to the entrances of the channels, were subject to external forces, a setup which might artificially affect the number of water molecules permeating the channel. This shortcoming was overcome later [5] through application of external forces only to water molecules in region III (Fig. 3), which leaves regions I and II under uniform hydrostatic pressures, and, hence, represents experimental conditions more closely.

In order to keep the membrane in place, one can either apply constant counter forces on the membrane to balance the effect of hydrostatic pressure gradients experienced by the membrane [4], or constrain the membrane in the z-direction to prevent an overall translation of the system. The latter is superior, because the number of water molecules (n) in region III, and, therefore, the total external force to water (nf), experience slight fluctuations during the simulation, and application of a fixed counter force on the membrane may not always exactly balance nf. Moreover, for very long simulations, applying constraints can also eliminate drifting of the membrane along the z-direction that may happen due to thermal motion. Too strong constraints, however, may restrict the dynamics of channel lining groups, which might, particularly in proteins, influence the kinetics of water transport, and one must carefully choose the constraints as to minimize this undesired effect.

An interesting method, which we refer to as the "two-chamber setup", has also been used to study osmotically driven water flow in MD simulations [25], where the unit cell consists of two membranes and two water layers containing different concentrations of solutes. We chose our proposed method rather than the two-chamber setup for two reasons. First, in order to observe on the ns time scale a statistically significant water flux through channels, one has to induce in the two-chamber setup a large chemical potential difference ($\Delta\mu$) of water. However, it is noteworthy that Eq. (10) is valid only for dilute solutions; when the solute concentration is high, $\Delta\mu$ is no longer linearly proportional to the concentration difference. In contrast, in our method, $\Delta\mu$ can be linearly controlled (see Eq. (26)). Second, the osmotic water flux in the two-chamber setup will decrease with time and eventually stop [25], while application of a hydrostatic pressure gradient maintains a stationary flux that permits sampling for as long as one can afford.

7. Calculation of Water Permeability of Aquaporins

As discussed earlier, using the CTRW model [24], one can demonstrate that p_{f} and p_{d} of a single-file water channel are related, but differ in value. Equilibrium MD simulations yield the p_{d} value, and applying hydrostatic pressure

differences across the membrane allows one to determine p_f of membrane channels from MD simulations. We will now present the application of the described method to the example of a real biological channel, namely AQP1. Pressure-induced water permeation will be used to determine the channel's p_f value, which, as we will see, is found to agree well with experimental measurements. The simulations presented in this section are taken from [5].

The AQP1 [9] tetramer was embedded in a POPE lipid bilayer and solvated by adding layers of water molecules on both sides of the membrane. The whole system (shown in Fig. 4) contains 81 065 atoms. The system was first equilibrated for 500 ps with the protein fixed, under constant temperature (310 K) and constant pressure (1 atm) conditions. Then the protein was released and another 450 ps equilibration performed.

Starting from the last frame of the equilibration, four simulations were initiated. In these simulations (sim1, sim2, sim3 and sim4), a constant force (f) was applied to the oxygen atoms of water molecules in region III, defined as a 7.7 Å-thick layer (shown in Fig. 4) in our system, to induce a pressure difference across the membrane. In principle, the position and thickness of region III can be arbitrarily defined and should not affect the results, as long as the induced pressure difference is set to the same value (by choosing a proper f); in practice, one would partition the bulk water in such a way that

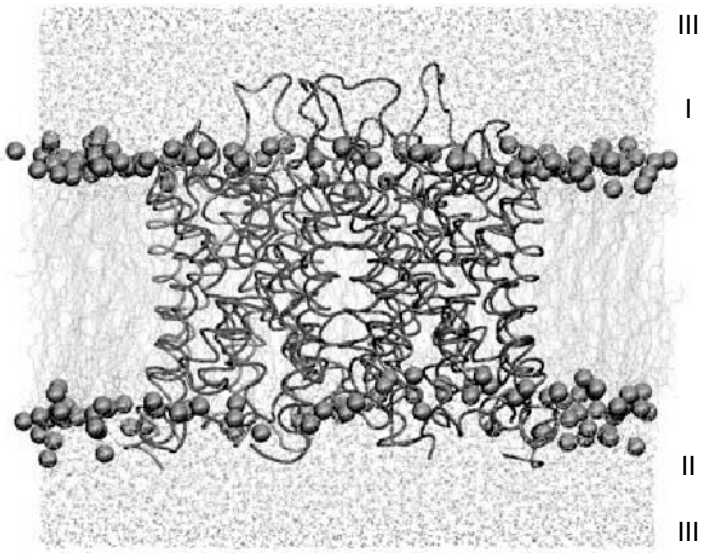

Figure 4. Side view of the unit cell including the AQP1 tetramer (tuberepresentation), and lipid and water molecules (line representation). Hydrogen atoms of lipids are not shown and the phosphorus atoms are drawn as vdW spheres. Water molecules in region III (see Fig. 3) are drawn in a slightly darker shade.

each of the three regions (I, II, III) has a sufficiently large thickness (relative to the diameter of a water molecule). The constant forces used in the four simulations differ in their direction or magnitude, generating four pressure differences, as summarized in Table 1. The simulations were performed under constant temperature (310 K) and constant volume conditions.

As mentioned earlier, the membrane needs to be constrained to prevent the overall translocation of the system under the external forces. This was done by applying harmonic constraints to the C_α atoms of the protein and the phosphorus atoms of the lipid molecules, with spring constants of 0.12 kcal/mol/Å^2 and 0.8 kcal/mol/Å^2, respectively. These spring constants are chosen to fully balance the external forces when the whole membrane is displaced by about Å along z from its reference position under a pressure difference of 200 MPa (as in sim1 and sim4). The constraints are applied only in the z-direction, and all atoms are free to move in the x- and y-directions. Note that the constraints on the protein are fairly weak and act only on the backbone C_α atoms; therefore, significant flexibility of protein side chains, which may influence the kinetics of water permeation, was maintained during the simulations.

All simulations were performed using the CHARMM27 force field [26], the TIP3P water model, and the MD program NAMD2 [27]. Full electrostatics was employed using the Particle Mesh Ewald (PME) method [28]. Simulations sim1, sim2, sim3 and sim4 were each run for 5 ns, with the first 1 ns discarded and the remaining 4 ns used for analysis. 1 ns of simulation took 22.4 h on 128 1-GHz Alpha processors.

During the simulations, the water density distribution in regions I, II, and III exhibited different patterns, as shown in Fig. 5, where the dashed lines are the boundaries separating these regions. In region III, where the external forces are applied, a gradient of water density is observed; in regions I and II, the density of water is roughly constant, indicating that the hydrostatic pressure in these regions is uniform. The water density gradient in region III and, hence, the density difference between regions I and II, differ in the four

Table 1. Summary of the four simulations reported in this study[a]

	f (pN)	ΔP (MPa)	$\Delta\mu$ (kcal/mol)
sim1	−7.36	−195	−0.814
sim2	−3.68	−97	−0.407
sim3	3.68	97	0.407
sim4	7.36	195	0.814

[a]The thickness of region III is d = 7.68 Å, containing on average 2470 water molecules. f is the constant force applied on individual water molecules. The area of the membrane in the unit cell is $A = 9.35 \times 10^{-17}$m^2. The induced pressure difference ΔP and chemical potential difference $\Delta\mu$ of water are calculated according to Eqs. (25) and (26), respectively.

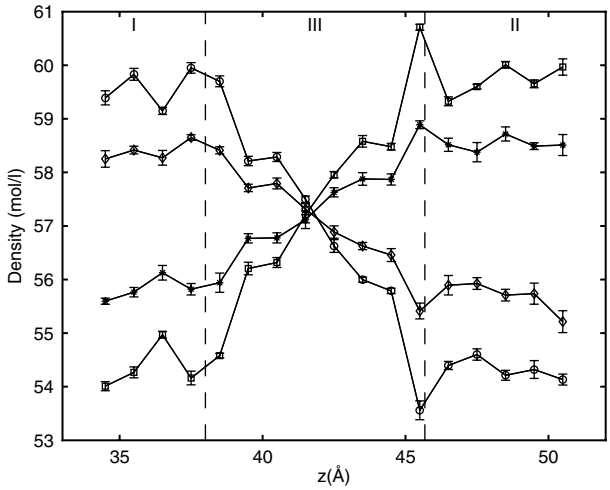

Figure 5. Water density distribution along the z-direction in region III (bracketed by the dashed lines) and part of regions I and II. Data points marked by circles, diamonds, stars, and squares represent sim1, sim2, sim3, and sim4, respectively. The density is measured by averaging the number of water molecules within a 1 Å-thick slab over the last 4 ns of each trajectory.

simulations. From the observed water density difference and the calculated pressure difference (see Table 1) in these simulations, the compressibility of water is estimated to be 4.9×10^{-5} atm, which is in satisfactory agreement with its experimental value of 4.5×10^{-5} atm [19].

Water molecules in the channels were usually found in the single-file configuration (as shown in Fig. 6a) and moved concertedly during the simulations (Fig. 6b). Occasionally, larger number of water molecules were accommodated in the channel, or the water file appeared broken in part of the channel. Nevertheless, the CTRW model can be used to provide a simplified quantitative description of water movement in AQP1 channels, as demonstrated in [5].

The net water fluxes, directly determined from the simulations, are shown in Table 2. These values are plotted vs. the applied pressure difference in Fig. 7. From their best-fit slope, and according to Eqs. (1) and (15), the osmotic permeability was determined to be $p_f = (7.1 \pm 0.9) \times 10^{-14}$ cm^3/s. Different experiments have reported p_f values for AQP1 monomers in the range of 1–16 $\times 10^{-14}$ cm ^{3}/s, the variation being probably due to uncertainties in the number of channels per unit membrane area; typically referenced p_f values range from 5.43×10^{-14} cm^3/s [29] to 11.7×10^{-14}cm^3/s [21]. In light of this, the p_f value calculated from our simulations agrees satisfactorily with experiments.

In equilibrium MD simulations of AQP1, a total of 16 permeation events (in four AQP1 monomers in either direction) were observed in 10 ns [11]. Therefore, the rate of uni-directional permeation events in a monomer is

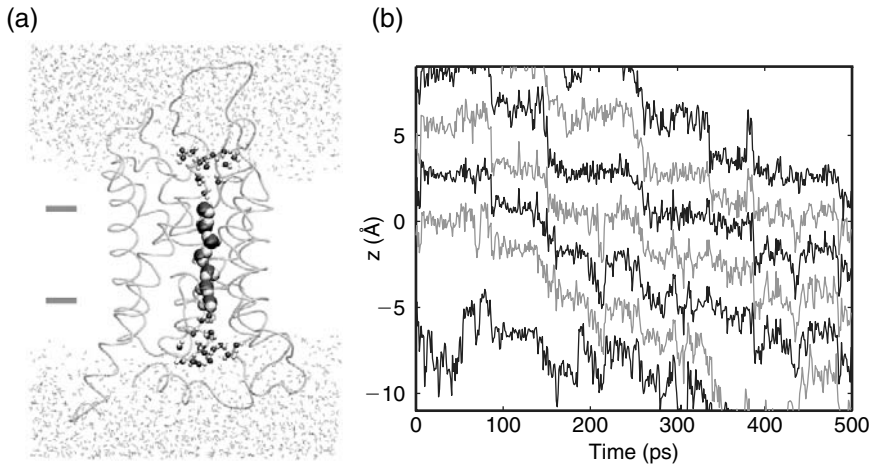

Figure 6. (a) An AQP1 monomer with channel water and nearby bulk water. Water molecules in the constriction (single-file) region, the vestibules of the channel, and in the bulk are rendered in vdW, CPK and line representations, respectively. (b) Trajectories (from sim1) of seven water molecules in the constriction region during 500 ps.

Table 2. Water flux observed in the four simulations[a]

	Water count/4 ns				Flux (#/ns)	
	M1	M2	M3	M4	Mean	SD
sim1	−13.5	−14.5	−15	−17.5	−3.8	0.4
sim2	−9.5	−6	−1	−12.5	−1.8	1.2
sim3	11.5	8.5	5	8	2.1	0.7
sim4	11.5	9	10.5	7	2.4	0.5

[a] To obtain the net water transfer through a channel, a plane normal to its axis is defined, and when a water molecule crosses the plane, a count of +1 or −1 is accumulated, depending on its crossing direction. Two such planes were defined in the central part of the channel, and the average of their net counts is listed as the water count of the channel. The mean and standard deviation (SD) of the flux were calculated from the water counts of the four AQP1 monomers (M1 to M4) during 4 ns.

$q_0 = 0.2\,H_2O$/ns. According to Eq. (3), this q_0 value translates into a diffusion permeability of $p_d = 6.0 \times 10^{-15}$ cm^3/s. Using this p_d value and the calculated p_f value of this study, one obtains a p_f/p_d ratio of 11.9, in good agreement with the experimentally measured ratio of 13.2 for AQP1 [20]. The ratio corresponds to the number of effective steps in which a water molecule needs to participate to cross AQP1.

The number (∼12) of effective steps in a complete permeation event should be interpreted as follows. In the bulk, water conduction is essentially uncorrelated, i.e., the bulk phase does not contribute to the p_f/p_d ratio. In the

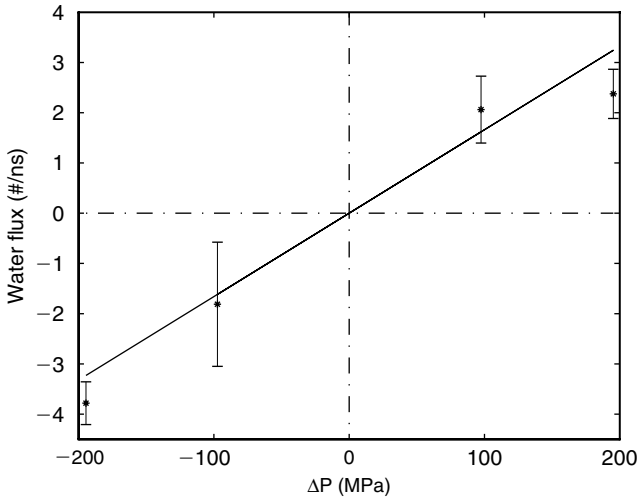

Figure 7. Relation of water flux and the applied pressure gradient. Values of pressure differences and water fluxes are taken from Tables 1 and 2, respectively. A line with the best-fit slope for the four data points is also shown in the figure.

constriction region of the channel, however, on average $N = 7$ water molecules move essentially in single file, i.e., in a correlated and concerted fashion, such that $N + 1 = 8$ steps are needed to transport a water molecule through. Water molecules in the vestibules (also shown in Fig. 6a) at the termini of the channel are not forming a single file, but nevertheless move in a somewhat concerted fashion, accounting for the remainder of the p_f/p_d ratio.

For AQP1, the average number of water molecules in the single-file region is about 7 corresponding to a pt/pd ratio of 8, but the experimentally measured ratio of p_f/p_d is 13.2 [20]. In order to understand the difference, we note that water molecules in an AQP1 channel may occasionally deviate from the single-file configuration due to conformational fluctuation of the protein. Furthermore, the behavior of water in the vestibule regions of AQP channels [3, 13, 30] suggests that the single-file model is too simple and that water transport effectively involves vestibular water at the channel entrances, such that the latter water cannot be counted as bulk water (see Fig. 6a).

8. Nanotube Simulations and the Collective Diffusion Model

In order to illustrate the validity of the collective diffusion model we consider MD simulations performed on two channels [23], denoted as a and b, and shown in Fig. 8. The simulations and systems results presented in this section

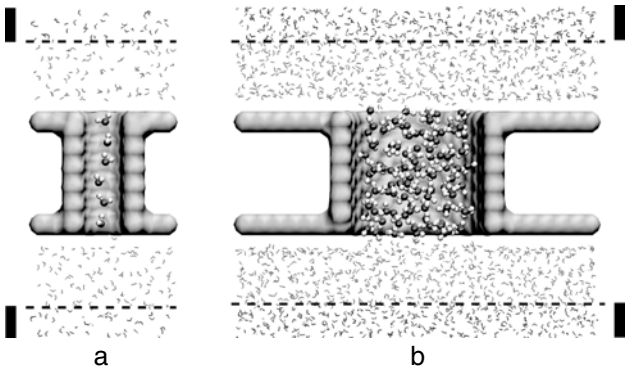

Figure 8. Side view of the unit cells in systems a andb, with dimensions of 18.0 Å × 18.0 Å × 41.4 Å and 46.0 Å × 46.0 Å × 42.1 Å, respectively. Half of the CNT channels and the membranes are removed in order to reveal water molecules in the channels. The dashed lines and the bars indicate the layers where constant forces were applied to the water molecules in nonequilibrium simulations (see text).

are taken from [23]. In each system, two layers of carbon atoms mimicking a membrane partition the bulk water and a CNT serves as a water channel. The CNT in system a is of (6,6) armchair type with a C–C diameter of ∼8 Å. Previous simulations [17, 18] showed that this CNT conducts water strictly in single-file manner. The CNT in system b is of (15,15) armchair type with a C–C diameter of ∼20 Å, and with disordered, bulk-like water molecules in it. Systems a and b contain 276 (∼5 in pore) and 1923 (∼90 in pore) water molecules, respectively. The length of the channel is $L = 13.2$ Å in both systems.

All nanotube simulations were performed under periodic boundary conditions with constant volume. The temperature was kept constant (T = 300 K) by Langevin dynamics with a damping coefficient of 5/ps. The CNT and the membrane were fixed in all simulations. The TIP3P model was used for water molecules. We employed the MD program NAMD2 [27] for the simulations, with full electrostatics calculated by the PME method. The channels were fixed and kept rigid throughout the simulations. This ensured that the channel maintains its structure under the large pressure from bulk water molecules.

Equilibrium MD simulations of 40 ns and 20 ns were performed on systems a and b, respectively, with coordinates recorded every picosecond. We took the sum of one-dimensional displacements of all water molecules in the channel, divided by L, as the displacement Δn in each picosecond (cf. Eq. (18)). If a water molecule enters or exits the channel within a picosecond, only the portion of its displacement within the channel contributes to the sum. The trajectories of $n(t)$, as shown in Fig. 9, were obtained by summing up (integrating) the Δn values as explained above. The mean square deviation (MSD) of $n(t)$

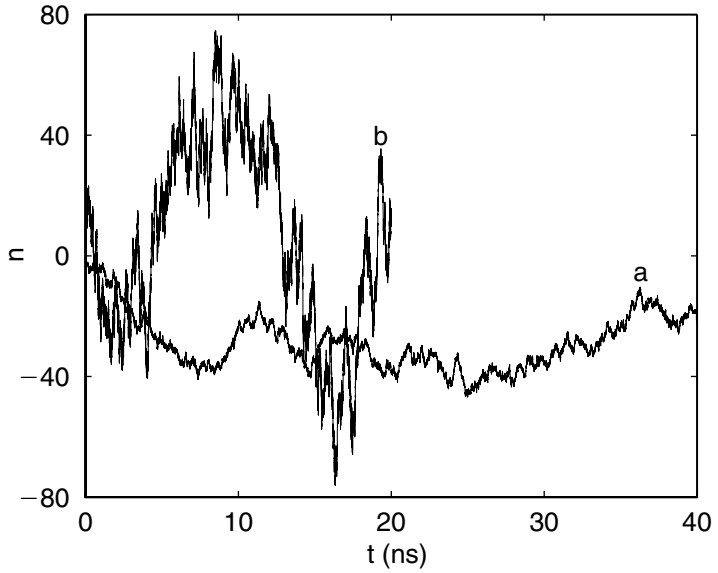

Figure 9. Trajectories of n for equilibrium MD simulations of systems a and b.

for each system is presented in Fig. 10. According to Eq. (20), the diffusion coefficient D_n is one-half of the slope of the MSD–t curve. From the best-fit slopes, the D_n values were determined to be (16.5 ± 2.1)/ns and (524 ± 40)/ns for systems a and b, respectively.

In order to test the key aspect of the collective diffusion model, namely, Eq. (23), we need to perform nonequilibrium simulations in the presence of a chemical potential difference ($\Delta\mu$) of water across the membrane. This was achieved by application of a hydrostatic pressure difference, which corresponds to a chemical potential difference $\Delta\mu = fd$ across the membrane. The defined layers in systems a and b are shown in Fig. 8, with thicknesses $d = 7.4$ and 8.1 Å, respectively. By choosing a proper f, one can select any desired value for $\Delta\mu$. For each system, we performed six nonequilibrium simulations, with $\Delta\mu$ set to $0.2\,k_BT$, $0.5\,k_BT$, $1\,k_BT$, $2\,k_BT$, $5\,k_BT$, and $10\,k_BT$. The simulation times (1–40 ns) varied in different simulations, but were long enough to observe a net transport of at least 100 water molecules in each case.

Figure 11 shows both the predicted water fluxes (solid lines) from Eq. (23) and the observed water fluxes (squares) in the simulations, from which one can discern excellent agreements between predictions and simulations. The results demonstrate the validity of the collective diffusion model. It is remarkable that the water flux induced by a $\Delta\mu$ as large as $10\,k_BT$ can still be predicted by the D_n value determined from equilibrium simulations. In light of this, one is not surprised that the calculated osmotic permeability (p_f) of AQP1 obtained from

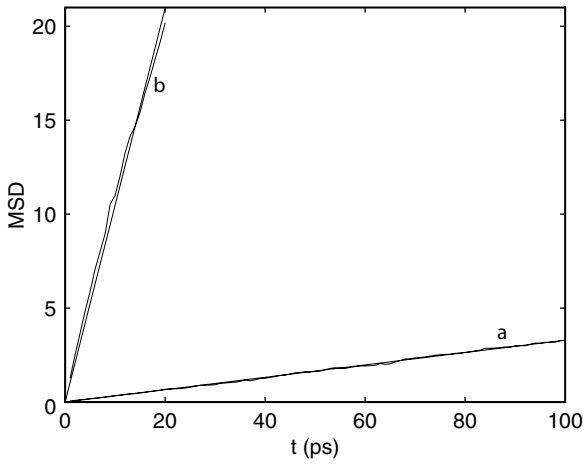

Figure 10. Mean square deviations (MSDs) of n for systems a and b. For each system, the trajectory $n(t)$ shown in Fig. 9 was evenly divided into M (400 for system a, 1000 for system b) short time-periods. $n(t)$ in each period was treated as an independent sub-trajectory $n_i^2(t)$, and was shifted so that $n_i(t)|_{t=0} = 0$. The average over $n_i(t)$ ($i = 1, \ldots, M$) was then taken as MSD(t). A line with the best-fit slope was superimposed on each MSD curve.

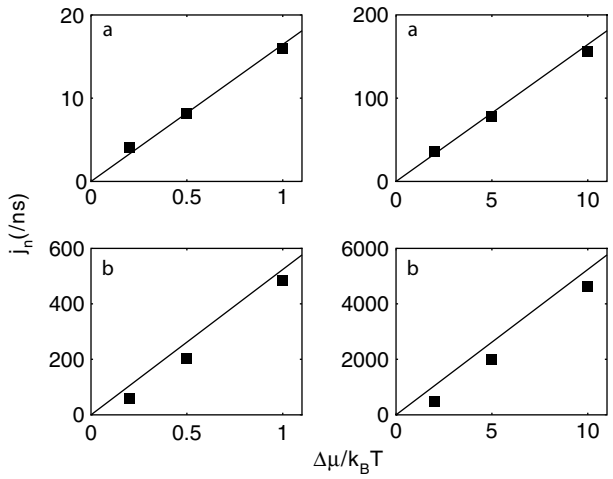

Figure 11. The dependence of water flux (j_n) on the chemical potential difference ($\Delta\mu$) of water. Each data point (marked as a square) represents the j_n value obtained from a nonequilibrium simulation, by dividing the total displacement of n in the simulation by the simulation time (cf. Eq. (19)). The solid lines show the j_n–$\Delta\mu$ relations predicted from Eq. (23), with $D_n = 16.5$ / ns for system a and $D_n = 524$ / ns for system b, both values being determined from the equilibrium simulations.

nonequilibrium simulations [5], which were reported in the previous section, agrees with the experimental data despite the fact that the $\Delta\mu$ values ($\sim 1\, k_B T$) in the simulations were much larger than experimental values (e.g., a solute concentration difference of 200 mM, as is typical in actual measurements, corresponds to a $\Delta\mu$ of $0.0036\, k_B T$).

In this section we have mainly focused on the collective movement of water inside the channel. The movement of individual water molecules also deserves attention. In particular, some water molecules may permeate all the way through the channel, an event described as a full permeation event. One can count the number of such permeation events in each direction in unit time, denoted as q_0, from equilibrium simulations. We observed q_0 values of about 3 and 110/ns from our equilibrium simulations for systems a and b, respectively. While the D_n value, which quantifies the collective water movement, determines the osmotic permeability p_f (see Eq. (24)), the q_0 value determines another experimental quantity for water channels, namely, the diffusion permeability p_d [5]. The ratio p_f/p_d is actually equal to D_n/q_0. We obtained D_n/q_0 ratios of 5.5 and 4.8 for systems a and b, respectively. The p_f/p_d ratio for a single-file channel can be interpreted as the number of effective steps a water molecule needs to take to completely cross the channel, i.e., the number of water molecules inside the channel plus 1 [5]; interestingly, despite the much larger number of water molecules in the pore region of system b, the p_f/p_d values for the two channels turned out to be similar. It is of interest to determine this ratio for different types of water channels in future studies.

The collective diffusion model establishes a quantitative relationship between the spontaneous water transport at equilibrium and the stationary water flux under nonequilibrium conditions. Using this model, p_f can be determined readily from equilibrium MD simulations. Since the model does not make specific assumptions on water channels, it can be used to characterize water permeation in any channel.

9. Outlook

Biological water channels, even though only recently discovered, have evolved rapidly to a level of rather complete characterization, both through observation and theory. A key reason for the successful investigations was the fact that the structure of the channel has been solved for key members of the AQP family. Other reasons for the success are the relatively simple function, water transport, the lack of significant motion needed for function, and the related very rigid structure of water channel proteins.

Yet, there are still fascinating research problems connected with water channels. Most pressing is an understanding of the mechanism of proton exclusion that is vital for the biological function, since the channels must not

dissipate cell membrane potentials. Much success has been achieved recently [3, 31–34].

Another interesting aspect of water channel research is to develop an understanding of the diversity of water channels in the whole kingdom of life. Humans have 11 different AQPs [34] in various tissues, some being pure water channels, others being water as well as glycerol channels. The differences in the human AQPs might be related to their function, e.g., possibly to their different ability to gate the channel, but more likely connected with the transport, storage, and deployment of the channels in cells, e.g., as controlled through the antidiuretic hormone. Likewise, existence of many different AQPs in other species, such as plants, yeast, and bacteria, and their involvement in membrane transport of materials ranging from O_2 and CO_2 gases to substrates like nitrate pose important questions in terms of their selectivity that need to be understood.

A fascinating opportunity for the study of AQPs has been opened up recently through the solvation of the structures of both an aqualglyceroprin (GlpF) and a pure water channel (AqpZ) for a single organism, namely, *E. coli* [10, 36]. A comparison of the two structures provides a fundamental chance to understand the design of this important class of membrane channels in terms of selectivity, transport rates, and role in the survival of cells.

Acknowledgments

We acknowledge grants from the National Institutes of Health NIH P41-RR05969 and R01-GM067887 and from the National Science Foundation NSF CCR 02-10843. The authors also acknowledge computer time provided at the NSF centers by the grant NRAC MCA93S028. F.Z. acknowledges a graduate fellowship awarded by the UIUC Beckman Institute. Molecular images in this paper were generated with the molecular graphics program VMD [37].

References

[1] A. Finkelstein, *Water Movement Through Lipid Bilayers, Pores, and Plasma Membranes*, John Wiley & Sons, New York, 1987.

[2] F. Zhu, E. Tajkhorshid, and K. Schulten, "Molecular dynamics study of aquaporin-1 water channel in a lipid bilayer," *FEBS Lett.*, 504, 212–218, 2001.

[3] E. Tajkhorshid, P. Nollert, M.Ø. Jensen, L.J.W. Miercke, J. O'Connell, R.M. Stroud, and K. Schulten, "Control of the selectivity of the aquaporin water channel family by global orientational tuning," *Science*, 296, 525–530, 2002.

[4] F. Zhu, E. Tajkhorshid, and K. Schulten, "Pressure-induced water transport in membrane channels studied by molecular dynamics," *Biophys. J.*, 83, 154–160, 2002.

[5] F. Zhu, E. Tajkhorshid, and K. Schulten, "Theory and simulation of water permeation in aquaporin-1," *Biophys. J.*, 86, 50–57, 2004.
[6] A.J. Yool and A.M. Weinstein, "New roles for old holes: ion channel function in aquaporin-1," *News Physio. Sci.*, 17, 68–72, 2002.
[7] K. Murata, K. Mitsuoka, T. Hirai, T. Walz, P. Agre, J.B. Heymann, A. Engel, and Y. Fujiyoshi, "Structural determinants of water permeation through aquaporin-1," *Nature*, 407, 599–605, 2000.
[8] G. Ren, V.S. Reddy, A. Cheng, P. Melnyk, and A.K. Mitra, "Visualization of a water-selective pore by electron crystallography in vitreous ice," *Proc. Natl. Acad. Sci. U.S.A.*, 98, 1398–1403, 2001.
[9] H. Sui, B.-G. Han, J.K. Lee, P. Walian, and B.K. Jap, "Structural basis of water-specific transport through the AQP1 water channel," *Nature*, 414, 872–878, 2001.
[10] D. Fu, A. Libson, L.J.W. Miercke, C. Weitzman, P. Nollert, J. Krucinski, and R.M. Stroud, "Structure of a glycerol conducting channel and the basis for its selectivity," *Science*, 290, 481–486, 2000.
[11] B.L. de Groot and H. Grubmüller, "Water permeation across biological membranes: mechanism and dynamics of aquaporin-1 and GlpF," *Science*, 294, 2353–2357, 2001.
[12] M.Ø. Jensen, E. Tajkhorshid, and K. Schulten, "The mechanism of glycerol conduction in aquaglyceroporins," *Structure*, 9, 1083–1093, 2001.
[13] M.Ø. Jensen, S. Park, E. Tajkhorshid, and K. Schulten, "Energetics of glycerol conduction through aquaglyceroporin GlpF," *Proc. Natl. Acad. Sci. U.S.A.*, 99, 6731–6736, 2002.
[14] M.Ø. Jensen, E. Tajkhorshid, and K. Schulten, "Electrostatic tuning of permeation and selectivity in aquaporin water channels," *Biophys. J.*, 85, 2884–2899, 2003.
[15] S. Iijima, "Helical microtubules of graphitic carbon," *Nature*, 354, 56–58, 1991.
[16] R. Saito, G. Dresselhaus, and M.S. Dresselhaus, *Physcial Properties of Carbon Nanotubes*, Imperial College Press, 1998.
[17] G. Hummer, J.C. Rasaiah, and J.P. Noworyta, "Water conduction through the hydrophobic channel of a carbon nanotube," *Nature*, 414, 188–190, 2001.
[18] F. Zhu and K. Schulten, "Water and proton conduction through carbon nanotubes as models for biological channels," *Biophys. J.*, 85, 236–244, 2003.
[19] N. Sperelakis, *Cell Physiology Source Book*, Academic Press, San Diego, 1998.
[20] J.C. Mathai, S. Mori, B.L. Smith, G.M. Preston, N. Mohandas, M. Collins, P.C.M. van Zijl, M.L. Zeidel, and P. Agre, "Functional analysis of aquaporin-1 deficient red cells," *J. Biol. Chem.*, 271, 1309–1313, 1996.
[21] M.L. Zeidel, S.V. Ambudkar, B.L. Smith, and P. Agre, "Reconstitution of functional water channels in liposomes containing purified red cell CHIP28 protein, *Biochemistry*, 31, 7436–7440, 1992.
[22] P. Pohl, S.M. Saparov, M.J. Borgnia, and P. Agre, "Highly selective water channel activity measured by voltage clamp: analysis of planar lipid bilayers reconstituted with purified AqpZ," *Proc. Natl. Acad. Sci. U.S.A.*, 98, 9624–9629, 2001.
[23] F. Zhu, E. Tajkhorshid, and K. Schulten, "Collective diffusion model for water permeation through microscopic channels," *Phys. Rev. Lett.*, 2004, submitted.
[24] A. Berezhkovskii and G. Hummer, "Single-file transport of water molecules through a carbon nanotube," *Phys. Rev. Lett.*, 89, 064503, 2002.
[25] A. Kalra, S. Garde, and G. Hummer, "Osmotic water transport through carbon nanotube membranes," *Proc. Natl. Acad. Sci.U.S.A.*, 100, 10175–10180, 2003.
[26] A.D. MacKerell Jr., D. Bashford, M. Bellott *et al.*, "All-hydrogen empirical potential for molecular modeling and dynamics studies of proteins using the CHARMM22 force field," *J. Phys. Chem. B*, 102, 3586–3616, 1998.

[27] L. Kalé, R. Skeel, M. Bhandarkar, R. Brunner, A. Gursoy, N. Krawetz, J. Phillips, A. Shinozaki, K. Varadarajan, and K. Schulten, "NAMD2: greater scalability for parallel molecular dynamics," *J. Comp. Phys.*, 151, 283–312, 1999.

[28] U. Essmann, L. Perera, M.L. Berkowitz, T. Darden, H. Lee, and L.G. Pedersen, "A smooth particle mesh Ewald method," *J. Chem. Phys.*, 103, 8577–8593, 1995.

[29] T. Walz, B.L. Smith, M.L. Zeidel, A. Engel, and P. Agre, "Biologically active two-dimensional crystals of aquaporin CHIP," *J. Biol. Chem.*, 269, 1583–1586, 1994.

[30] D. Lu, P. Grayson, and K. Schulten, "Glycerol conductance and physical asymmetry of the *Escherichia coli* glycerol facilitator GlpF," *Biophys. J.*, 85, 2977–2987, 2003.

[31] B.L. de Groot, T. Frigato, V. Helms, and H. Grubmüller, "The mechanism of proton exclusion in the aquaporin-1 water channe," *J. Mol. Biol.*, 333, 279–293, 2003.

[32] A. Burykin and A. Warshel, "What really prevents proton transport through aquaporins," *Biophys. J.*, 85, 3696–3706, 2003.

[33] N. Chakrabarti, E. Tajkhorshid, B. Roux, and R. Pomès, "Molecular basis of proton blockage in aquaporins," *Structure*, 12, 65–74, 2004.

[34] B. Ilan, E. Tajkhorshid, K. Schulten, and G.A. Voth, "The mechanism of proton exclusion in aquaporin channels," *Proteins: Struct. Func. Bioinf.*, 55, 223–228, 2004.

[35] J.B. Heymann and A. Engel, "Aquaporins: phylogeny, structure, and physiology of water channels," *News Physio. Sci.*, 14, 187–193, 1999.

[36] D.F. Savage, P.F. Egea, Y. Robles-Colmenares, J.D. O'Connell III, and R.M. Stroud, "Architecture and selectivity in aquaporins: 2.5 Å x-ray structure of aquaporin Z," *PLoS Biol.*, 1, 334–340, 2003.

[37] W. Humphrey, A. Dalke, and K. Schulten, "VMD – visual molecular dynamics," *J. Mol. Graphics*, 14, 33–38, 1996.